



Using volume-weighted average wood specific gravity of trees reduces bias in aboveground biomass predictions from forest volume data



Le Bienfaiteur Takougoum Sagang^{a,c,*}, Stéphane Takoudjou Momo^{a,b}, Moses Bakonck Libalah^{a,b}, Vivien Rossi^d, Noël Fonton^d, Gislain II Mofack^a, Narcisse Guy Kamdem^a, Victor François Nguetsop^c, Bonaventure Sonké^a, Ploton Pierre^b, Nicolas Barbier^b

^a Plant Systematic and Ecology Laboratory (LaBosystE), Department of Biology, Higher Teachers' Training College, University of Yaoundé I, P.O. Box 047, Yaoundé, Cameroon

^b AMAP, IRD, CNRS, INRA, Univ Montpellier, CIRAD, Montpellier, France

^c Laboratory of Applied Botany, Faculty of Sciences, University of Dschang, Dschang, Cameroon

^d Commission des Forêts d'Afrique Centrale (COMIFAC), Yaoundé BP 2572, Cameroon

ARTICLE INFO

Keywords:

Wood specific gravity
Terrestrial LiDAR
Aboveground biomass
Linear model
Error propagation
Cameroon eastern forest
Remote sensing

ABSTRACT

With the improvement of remote sensing techniques for forest inventory application such as terrestrial LiDAR, tree volume can now be measured directly, without resorting to allometric equations. However, wood specific gravity (WSG) remains a crucial factor for converting these precise volume measurements into unbiased biomass estimates. In addition to this WSG values obtained from samples collected at the base of the tree (WSG_{Base}) or from global repositories such as Dryad (WSG_{Dryad}) can be substantially biased relative to the overall tree value. Our aim was to assess and mitigate error propagation at tree and stand level using a pragmatic approach that could be generalized to National Forest Inventories or other carbon assessment efforts based on measured volumetric data. In the semi-deciduous forests of Eastern Cameroon, we destructively sampled 130 trees belonging to 15 species mostly represented by large trees (up to 45 Mg). We also used stand-level dendrometric parameters from 21 1-ha plots inventoried in the same area to propagate the tree-level bias at the plot level. A new descriptor, volume average-weighted WSG ($WWSG$) of the tree was computed by weighting the WSG of tree compartments by their relative volume prior to summing at tree level. As $WWSG$ cannot be assessed non-destructively, linear models were adjusted to predict field $WWSG$ and revealed that a combination of WSG_{Dryad} , diameter at breast height (DBH) and species stem morphology (S_m) were significant predictors explaining together 72% of $WWSG$ variation. At tree level, estimating tree aboveground biomass using WSG_{Base} and WSG_{Dryad} yielded overestimations of 10% and 7% respectively whereas predicted $WWSG$ only produced an underestimation of less than 1%. At stand-level, WSG_{Base} and WSG_{Dryad} gave an average simulated bias of 9% (S.D. = ± 7) and 3% (S.D. = ± 7) respectively whereas predicted $WWSG$ reduced the bias by up to 0.1% (S.D. = ± 8). We also observed that the stand-level bias obtained with WSG_{Base} and WSG_{Dryad} decreased with total plot size and plot area. The systematic bias induced by WSG_{Base} and WSG_{Dryad} for biomass estimations using measured volumes are clearly not negligible but yet generally overlooked. A simple corrective approach such as the one proposed with our predictive $WWSG$ model is liable to improve the precision of remote sensing-based approaches for broader scale biomass estimations.

1. Introduction

Above ground biomass in tropical forests constitute a major component of the global carbon cycle, but our ability to measure and predict its carbon stocks and dynamics is limited (Chave et al., 2014; Fayolle et al., 2014). In an effort to conserve tropical forests, the United Nations Framework Convention on Climate Change (UNFCCC) has

developed a mechanism called Reducing Emissions from Deforestation and Forest Degradation in tropical countries (REDD+). There is high interest in seeing such initiatives take form, but a key limitation for successful implementation of REDD+ lies in the lack of reliable methods for quantifying forest aboveground biomass (AGB) over large areas (Gibbs et al., 2007; Joseph et al., 2013). Sample-based (Maniatis et al., 2011) or remote sensing (RS) based (Ploton et al., 2017) methods

* Corresponding author at: PO Box 47, Yaoundé, Cameroon.

E-mail address: sagang.bienfaiteur@yahoo.fr (L.B.T. Sagang).

both rely on AGB estimations in forest sample plots to derive larger scale estimations. [Chave et al. \(2004\)](#) reported four types of uncertainties that could lead to statistical error in plot AGB estimates: (i) error due to tree measurement; (ii) error due to the choice of an allometric model relating AGB to other tree dimensions; (iii) sampling uncertainty, related to the size of the study plot; (iv) representativeness of a network of small plots across a vast forest landscape. Most allometric models for biomass estimation are based on three variables: tree diameter at breast height, tree height and wood specific gravity (*WSG*). The latter refers to the oven-dried mass of a wood sample divided by its green volume ([Williamson and Wiemann, 2010](#)). The two first variables serve to assess tree volume, while *WSG* allows converting this volume into a mass. Such models are in general calibrated using datasets (global) of destructively sampled trees, and only account for inter-specific differences through the *WSG* variable.

We see that any methodological advance that could improve the quality of volume and *WSG* estimations will help improve on (at least) the two first sources of statistical errors reported by [Chave et al. \(2004\)](#). With the increasing use of terrestrial LiDAR (Light Detection And Ranging) technologies for forestry applications, and the improvement of dedicated post-treatment algorithms, precise volume estimation at tree or even plot level are now at hand ([Ferraz et al., 2016](#); [Hackenberg et al., 2015](#); [Momo et al., 2017](#); [Stovall et al., 2017](#)). *A minima*, it will be possible to calibrate improved local allometric models, possibly accounting for structural variations between species or group of species. Eventually, it is expected that volumes will be directly extracted in routine from stand level scans, eliminating the need for allometric equations altogether ([Calders et al., 2015](#); [Disney et al., 2018](#)).

A crucial deadlock will remain, however, in the proper estimation of *WSG*. As *WSG* is rarely measured in the field and most studies ([Gourlet-Fleury et al., 2013](#); [Slik et al., 2013](#); [Bastin et al., 2015a](#); [Alvaro et al., 2017](#)) use species-average *WSG* values extracted from global repositories such as Dryad ([Chave et al., 2009](#); [Zanne et al., 2009](#)).

Yet, variation in *WSG* have been observed between individuals of the same species, along the length of individual tree trunk ([Wassenberg et al., 2015](#)), between trunk and branches ([Swenson and Enquist, 2008](#)) and from the heartwood to the bark ([Bastin et al., 2015b](#); [Nock et al., 2009](#); [Osazuwa-Peters et al., 2014](#)). As a consequence, the use of global repositories ([Zanne et al., 2009](#)) can lead to marked bias in local studies; for instance, an overestimation of the wood specific gravity of approximately 16% for the species community was obtained at the forest stand level in Madagascar ([Ramanantoandro et al., 2015](#)). When *WSG* is measured on site, it is generally via increment cores or wood disc samples collected at a given distance from the ground on the tree trunk. Therefore, such samples ignore any vertical variation that may exist within the tree. As global biomass allometric models were often calibrated using global *WSG* repositories, it is likely that systematic bias are in fact compensated through the parameters of the allometric equations themselves ([Picard et al., 2015](#)). As a result, predictions of allometric equations would not be biased, as long as the same repositories are used to provide *WSG* values, or as long as similarly biased protocols are used to obtain local *WSG* data (e.g. coring from the stem base). However, this would not be the case for approaches aiming at directly converting tree volumes (e.g. from terrestrial LiDAR data) into biomass. Here, *WSG* values for each tree compartment would be needed, or at least some tree level unbiased estimate of *WSG*. Ideally the estimator should be individual and account for vertical and radial variations. Approaching this ideal *WSG* would require taking complete increment cores (*i.e.* on at least a full diameter) in all tree compartments, followed by a volume-weighted average across compartments to obtain the tree-level volume weighted average *WSG* (*WWSG*), and this for each individual tree in a census. Obviously, the measurements required to reach this estimate can hardly be done on a standing tree, even less so in the frame of an operational, large scale application. The alternative is to look for simple correction models based on available *WSG* data (samples from the tree base or from

Dryad) and the morphology of trees.

In this study, we used a dataset of 130 trees destructively sampled in south-eastern Cameroon, with a consequent representation of large trees of *DBH* > 50 cm (52% of dataset) as well as 21 ha of forest inventory performed in the same location to (i) compare *WWSG* of trees with radially-averaged *WSG* extracted at breast height (*i.e.* 1.3 m) or with species-level *WSG* from Dryad repository; (ii) propose a new practical model to predict *WWSG*; and (iii) determine the bias yielded when estimating the aboveground biomass from those different *WSG* sources at the tree- and plot-level.

2. Material and methods

2.1. Study site

Data were collected in south-eastern Cameroon, within Forest Management Units (FMU) 10–051 and 10–53. The FMUs were located between 3°41'59" and 4°3'43"N, and 14°14'36" and 14°34'38"E. Average annual rainfall in the area varies between 1500 and 2000 mm, with three to four months of dry season (monthly rainfall < 100 mm). The average monthly temperature oscillates around 24 °C. Altitude varies between 600 and 760 m. The study site lies on Precambrian rocks with deep ferrallitic red to yellowish soils. *Terra firme* forests in the area are characterized by a mix of evergreen and semi-deciduous species dominated by *Cannabaceae* and *Malvaceae* families (hence "mixed-forests", [Letouzey, 1968](#)), and classified as semi-deciduous *Celtis* forests ([Fayolle et al., 2014](#)).

2.2. Species and trees sampling scheme

A total of 130 trees belonging to 15 species of 8 families were sampled ([Table 1](#)). Two selection criteria were employed: the first criterion included species relative abundance, which was obtained from existing forest management inventory data provided by the logging company; the second criterion was species mean *WSG*, derived from the Global Wood Density (GWD) database ([Zanne et al., 2009](#)) hereafter referred to as Dryad database. Each of the species retained were grouped into 6 *WSG* classes as follows: $\geq 0.4 \text{ g.cm}^{-3}$; [0.4–0.5]; [0.5–0.6]; [0.6–0.7]; [0.7–0.8] and $\geq 0.8 \text{ g.cm}^{-3}$. Trees were equally distributed into six diameter classes following a 10 cm interval class width from 10 to 50 cm, then three other diameter classes were used for large trees: [50–100] cm, [100–150] cm and > 150 cm. This methodology was established by the Regional Project for the strengthening of the institutional capacities on the REDD + initiative of the Commission of Central African Forest (PREREDD + – COMIFAC). Field campaigns were carried out from July 2015 to December 2016.

2.3. Field data collection

Before felling a tree, we measured the *DBH* at 1.3 m above the ground or 30 cm above the top of the last buttress.

After felling the tree, we measured trunk length (from ground-level up to lowest major living branch) and total tree length (up to the apparent crown tip) so to document species morphology: short-bole species (with the ratio between bole height and crown depth < 1) and tall-bole species (with the ratio between bole height and crown depth > 1; see [Appendix A](#)). Tree stump was then cut at ground level and the bole and crown were chunked into 1 to 2 m long sections as described by [Picard et al. \(2012\)](#). The tree was subdivided into seven compartments: 1 = stump; 2 = lower portion of the bole with buttresses; 3 = bole; 4 = large crown sections ($\varnothing \geq 20 \text{ cm}$, with \varnothing the basal section diameter); 5 = medium-sized crown sections ($5 \geq \varnothing < 20 \text{ cm}$); 6 = small crown sections ($\varnothing < 5 \text{ cm}$) and 7 = leaves and reproductive parts. For sections with $\varnothing \leq 70 \text{ cm}$, fresh masses were directly weighed in the field using a *Crane* electronic (3000 kg capacity, precision of 0.5 kg). For sections with $\varnothing > 70 \text{ cm}$, basal diameter, distal diameter and

Table 1

Description of the destructive dataset: Species stem morphology (S_m ; s = short-bole species; t = tall-bole species), number of sampled individuals (N), range of diameter at breast height (DBH), mean and standard deviation of WSG from (i) Dryad database (WSG_{Dryad}), (ii) destructive samples obtained at approximately breast height (WSG_{Base}) and (iii) destructive samples obtained on the entire tree and weighted by the volume of the compartment they came from ($WWSG$, see 2.5 for details).

Taxon	Family	S_m	N	DBH (cm) Min-Max	Wood specific gravity (kg m^{-3})				
					WWSG	S.D.	WSG_{Base}	S.D.	WSG_{Dryad}
<i>Annickia chlorantha</i>	Annonaceae	t	5	11.3–51	444.34	33.03	506.74	52.59	459.64
<i>Baphia leptobotrys</i>	Fabaceae	s	6	14.5–67	758.48	40.79	807.85	54.65	772.00
<i>Cylicodiscus gabunensis</i>	Fabaceae	t	11	13.5–159.5	645.25	97.33	796.23	101.85	778.84
<i>Duboscia macrocarpa</i>	Malvaceae	s	8	26.5–120.3	514.73	53.08	555.97	68.34	599.98
<i>Entandrophragma cylindricum</i>	Meliaceae	t	12	17.75–153.4	562.92	45.15	595.73	49.56	519.73
<i>Eribromao blongum</i>	Malvaceae	t	9	17.8–100.8	520.95	62.90	615.56	51.80	638.45
<i>Erythrophleum suaveolens</i>	Fabaceae	t	11	16.6–120.5	729.08	57.55	804.80	68.23	808.75
<i>Macaranga barteri</i>	Euphorbiaceae	s	5	17.2–53.5	348.04	19.79	361.74	48.06	381.79
<i>Mansonia altissima</i>	Malvaceae	t	7	19–74.56	509.06	20.44	529.70	30.65	723.23
<i>Pentaclethra macrophylla</i>	Fabaceae	s	5	11.5–112	669.96	185.86	805.69	207.85	702.48
<i>Petersianthus macrocarpus</i>	Lecythidaceae	t	10	14.7–74.5	548.70	53.08	601.44	58.98	608.25
<i>Pterocarpus soyauxii</i>	Fabaceae	t	10	11.6–94.3	559.02	50.46	692.19	43.98	626.89
<i>Pycnanthus angolensis</i>	Myristicaceae	t	8	14–95.2	387.33	44.75	450.51	32.03	408.90
<i>Terminalia superba</i>	Combretaceae	t	12	13–113.5	505.36	52.62	507.98	50.20	630.50
<i>Triplochiton scleroxylon</i>	Malvaceae	t	13	13.5–180.3	415.78	56.93	471.49	81.91	334.50

length were measured, so to derive fresh masses from sections' volume (see 2.4 – Volumes estimation) and specific gravity (see 2.4 – Wood specific gravity estimation). The fresh mass of leaves and reproductive parts was measured with a 300 kg capacity Crane electronic scale having a precision of 0.1 kg.

A 30–50 mm thick cross-sectional disc sample was extracted from each woody compartment of the tree. For discs with diameter greater than 20 cm, two opposite wedge-shaped samples were kept, stretching from the pith to the bark (according to the methodology defined in PREREDD+ project) to take into consideration radial variations (bark, sapwood and heartwood). Each wedge-shaped sample was immediately weighed in the field with a 5000 g capacity mechanic scale with a nominal precision of 25 g, whereas samples extracted from the crown were weighed with a 100 g capacity mechanic scale having a precision of 10 g. The samples were then sealed in a plastic bag to avoid water loss in preparation to determine the fresh volume in the laboratory.

2.4. Laboratory analyses

2.4.1. Volumes estimation

The volume of each woody compartment (V_c in m^3) was computed as the sum of compartment's sections volume (denoted v_s , in m^3). Each v_s was estimated using Smalian's formula (Pardé and Bouchon, 1988):

$$v_s = \{(B + b) \times 0.5\} \times L \quad (1)$$

where B is section's basal cross-sectional area (m^2), b is section's distal cross-sectional area (m^2) and L is section's length (m).

For correct determination of the cross-sectional area of sections with an irregular shape, the cross-sectional area was estimated by digitizing their photographic images (Vincke, 2011). Photographs were taken with a Nikon 5 X digital camera and the cross-sectional area was obtained using Qgis (version 2.8) as described by Daphné and Philippe (2014). Summing all compartments' volumes gave the total tree volume V_T (m^3);

$$V_T = \sum_{j=1}^n V_{c_{ij}} \quad (2)$$

where $V_{c_{ij}}$ is the volume of compartment j of tree i (m^3).

2.4.2. Wood specific gravity estimation

For each wood sample taken to the laboratory, the fresh mass and other weigh measurements were made with a Kern and Sohn electronic scale (5 kg capacity and precision of 0.001 g). The fresh volume was

determined by water displacement method (Vieilledent et al., 2012) following Archimedes Principle. The sample was then oven dried at 105 °C and its dry mass was obtained after three days or more, once mass measurements made every 6 h presented less than 1% differences. Sample WSG was calculated as its dry mass divided by its fresh volume. Moisture content (MC) was calculated as the difference between fresh and dry masses per unit fresh mass ($[\text{fresh mass} - \text{dry mass}]/\text{fresh mass}$).

2.5. Statistical analyses

For each woody compartment j , a volume-weighted wood specific gravity ($WWSG_j$) was calculated as the product of WSG_j (WSG_j is the average of the WSG of all the samples collected in that compartment j) and the compartment's volume V_{c_j} (m^3) relative to the entire tree volume, V_T (m^3):

$$WWSG_j = WSG_j \times \frac{V_{c_j}}{V_T} \quad (3)$$

A weighted average wood specific gravity at the tree level ($WWSG$) was then obtained by summing all $WWSG_j$ of that tree and was used for biomass predictions.

Estimating $WWSG$ was possible in this study thanks to a complete destructive sampling of tree, mass and volume estimation of all compartments, and laboratory measurements made on wood samples for all compartments. To allow the non-destructive estimation of $WWSG$, we calibrated linear prediction models using the tree diameter at breast height (DBH), the index of stem morphology (S_m); the species WSG from Dryad database (WSG_{Dryad}); and the individual WSG sampled at approximately breast height (WSG_{Base}) as independent variables and $WWSG$ as the dependent variable. Model selection was achieved using the Akaike's information criterion (AIC), the coefficient of determination (R^2) and the residual standard error (RSE) (Table 2).

Field AGB of each tree (AGB_{obs_i} in Mg), with $i = 1, \dots, 132$, was obtained by summing the dry masses of its different compartments. For woody compartments with fresh mass, the dry mass was obtained via the moisture content (dry mass = $[\text{fresh mass} - (\text{fresh mass} \times \text{MC})]$). For compartments with fresh volumes, their dry mass was obtained through the WSG of the compartment (dry weight = $V_{c_{ij}} \times WSG_j$). Leaves and reproductive organs were integrally weighed fresh in the field. Samples were collected from each tree and then oven dried at 60–70 °C to constant mass to derive the moisture content.

Estimated AGB (AGB_{est_i} in Mg) values were obtained by multiplying

Table 2

Linear prediction models for tree weighted average WSG (WWSG, kg m⁻³). Models were based on species WSG from Dryad database (WSG_{Dryad}, kg m⁻³), individual WSG from the base of the tree (WSG_{Base}, kg m⁻³) and structural parameters, namely diameter at breast height (DBH, cm) and species morphology (S_m). Classical model fit metrics (R², RSE, AIC) are provided along with model parameters and associated confidence intervals (95%).

Models	Model parameters				Model performance		
	a	b	c	d	R ²	RSE	AIC
1: WWSG = a + bWSG _{Base}	90.31 ^{***} (46.62 134)	0.74 ^{***} (0.67 0.81)			0.77 ^{***}	60.1	1459
2: WWSG = a + bWSG _{Base} + cDBH	58.13 ^{***} (15.7 100.57)	0.73 ^{***} (0.66 0.79)	0.64 ^{***} (0.38 0.91)		0.8 ^{***}	55.5	1439
3: WWSG = a + bWSG _{Base} + cDBH + dS _m	53.91 ^{***} (11.94 95.88)	0.72 ^{***} (0.66 0.79)	0.69 ^{***} (0.42 0.95)	27.81 ^{***} (3.09 52.53)	0.81 ^{***}	54.6	1436
4: WWSG = a + bWSG _{Dryad}	185.55 ^{***} (135.02 236.08)	0.6 ^{***} (0.52 0.68)			0.61 ^{***}	78.07	1529
5: WWSG = a + b WSG _{Dryad} + cDBH	115.8 ^{***} (65.99 165.6)	0.62 ^{***} (0.54 0.69)	1.03 ^{***} (0.7 1.35)		0.7 ^{***}	68.81	1496
6: WWSG = a + bWSG _{Dryad} + cDBH + dS _m	106.15 ^{***} (57.07 155.23)	0.61 ^{***} (0.54 0.68)	1.09 ^{***} (0.76 1.41)	42.11 ^{***} (11.84 72.39)	0.72 ^{***}	67.12	1491

Significance codes: 0 “***”, 0.001 “**”, 0.01 “*”, 0.05 “.”, 0.1 “ “.

the total tree volume (V_T) by either WSG_{Base}, WSG_{Dryad} or WWSG predicted from our linear models.

For each tree, AGB_{est} values were compared to AGB_{obs} (destructive) values based on the mean of individual relative bias s (in %), which are defined as follows:

$$s_i = \left(\frac{AGB_{est,i} - AGB_{obs,i}}{AGB_{obs,i}} \right) \times 100 \tag{4}$$

For a model to be unbiased we expect the mean s_i (noted s) to be close to zero.

Prediction errors at the tree level are expected to scale down at the plot level as negative and positive errors compensate, yet this compensation may be dependent on the actual tree mass distribution in the sample plot if individual error systematically varies with tree mass. To account for this source of error, we employed a simulation procedure (Monte Carlo scheme) which propagates tree level AGB errors to plot level (PAGB) in two steps (as in Ploton et al., 2016). We used census data from 21 1-ha plots installed in the study area (Libalah et al., 2018) to propagate AGB error from tree to plot level. Each plot was subdivided into 25 square quadrats of 20 m side and the DBH of all trees with DBH ≥ 10 cm were measured. In total, 9 780 individuals were censused, with a maximum observed DBH of 253 cm. The first step of the error propagation method consisted in attributing a simulated AGB value to each tree in a given quadrat (AGB_{sim}) corresponding to the actual AGB of a similar felled tree selected in the destructive database within the same DBH class value. The second step consisted in propagating individual errors from a given WSG source using the local distribution of s_i values as predicted by a Loess regression; for each AGB_{sim}, we randomly drew a S_{sim} value. Thus, we generated for each plot a realistic PAGB_{sim} (i.e., based on observed felled trees) with repeated realizations of a plot-level prediction error (in %) computed for n trees as follows.

$$S_{plot} = \frac{\sum_{i=1}^n (s_{sim}(i) \times AGB_{sim}(i))}{\sum_{i=1}^n AGB_{sim}(i)} \tag{5}$$

We computed the mean and the standard deviation of 1000 realizations of the plot-level prediction error for each of the simulated plots.

All analyses were performed in R statistical software (RStudio Team, 2016). The package PMCMR (Pohlert, 2016) was used for pairwise multiple comparisons of means.

3. Results

3.1. Comparison of wood specific gravity estimates

Comparing the three WSG estimates (WWSG, WSG_{Base} and WSG_{Dryad}) on 15 species, we found that significant differences could be detected at least between two WSG estimates for 11 species, with WWSG being significantly lower than WSG_{Base} and WSG_{Dryad} in 9 cases (Fig. 1). On average, WWSG was approximately 11% lower than WSG_{Base} and 8% lower than WSG_{Dryad}.

Mean WSG variation from the stump to the small branches (compartment 1 to 7) showed a general decrease in all species (Appendix B) except for *Macaranga barteri*, a light wooded species which presented the opposite variation pattern. When plotting the distribution of WWSG_j along tree species compartments (Appendix C), 11 species presented the highest WWSG_j value at the bole (compartment n°3) and the lowest WWSG_j in the stump (compartment n°1); the lower portion of the bole (compartment n°2) and the crown. In contrast, 4 species *Baphia leptobotrys*; *Duboscia macrocarpa*; *Macaranga. barteri* and *Pentaclethra macrophylla* presented highest WWSG_j values in the crown compartments.

3.2. Models to predict WWSG

Among the six linear models tested to predict WWSG, the model based on WSG_{Base}, DBH and S_m (ie. model 3) yielded the best performance (R² = 0.81, AIC = 1436, Table 2). Replacing WSG_{Base} in model 3 by WSG_{Dryad} (model 6) led to a decrease in model fit (R² = 0.72; AIC = 1491). As the purpose of the models is to propose one with variables that are easily accessible and knowing that WSG_{Base} is not always easy to measure on the field, we focused on model 6 as our reference model to predict WWSG.

3.3. Tree level biomass estimations

Estimating tree AGB_{est} (derived from compartments-level volumes and WSG) from total tree volume and WSG_{Base} led to tree AGB overestimation of up to 10% (RMSE = 1.8) as shown in Fig. 2a. Also, using WSG_{Dryad} led to tree AGB overestimation of up to 7% (RMSE = 3, Fig. 2b). However, using WWSG predicted from model 6 yielded the lowest bias (s = -1%, Fig. 2c).

3.4. Plot-level error propagation

Using the simulation procedure, we propagated AGB_{est} prediction error to 1-ha plots and observed that mean biases obtained when using

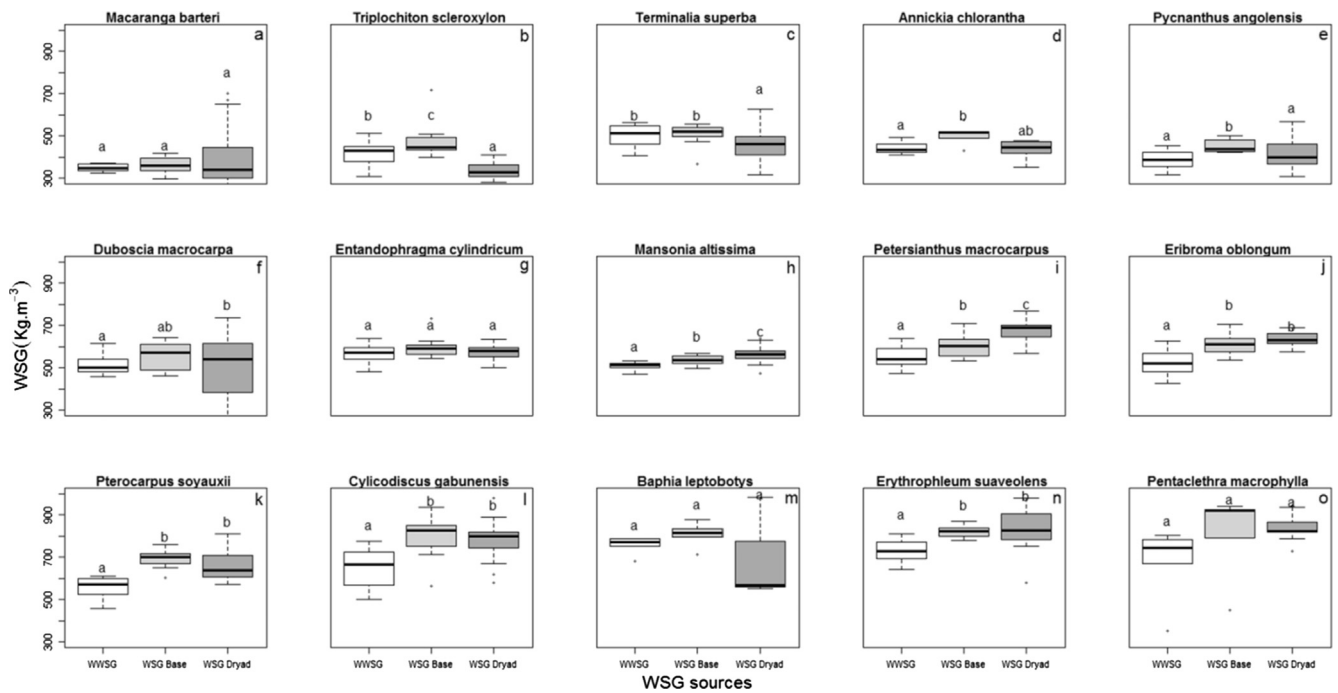


Fig. 1. Comparison between WWSG, WSG_{Base} and WSG_{Dryad} across 15 species. Letters above each box represent the results of Kruskal-Wallis post hoc test, with similar letters indicating that boxes mean values are not significantly different.

WSG_{Base} and WSG_{Dryad} were 9% (S.D. = ± 7; Fig. 3a) and 3% (S.D. = ± 7; Fig. 3b) respectively. Using WWSG predicted from model 6 reduced the bias by up to 0.1% (S.D. = ± 8; Fig. 3c) on estimated plot AGB.

When looking at the mean plot bias by WSG source against plot size (Fig. 4a), we observe a decreasing trend as the area of the plot increases up to a plot area of 0.64 ha from which the bias is constant (solid grey circles and solid black circles, respectively). When plotting AGB mean bias in function of the plot AGB (Fig. 4b), we observe a general decrease of bias as plot AGB increased for both WSG_{Base} and WSG_{Dryad} whereas the use of WWSG predicted with model 6 yielded a lower bias which did not appear to be correlated to plot AGB. Using WSG_{Base} and WSG_{Dryad} in estimating AGB in small plots (ie. ≤ 0.4 ha) led to an overestimation of up to 15% and 11% respectively; this bias is reduced to 3% with

WWSG predicted from model 6. This bias yielded with WWSG predicted from model 6 decreases down to 0.01% in 1 ha plots.

4. Discussion

Several studies have attempted to propose methods allowing to obtain more reliable estimation of tree-level WSG from field measurements (Bastin et al., 2015a,b; Deng et al., 2014; Osazuwa-Peters et al., 2014), with the aim to reduce bias in biomass assessment. However destructive datasets from tropical forests are relatively rare and not distributed evenly across regions. Most existing studies were furthermore limited to WSG variations in stems, and only a few studies (Henry et al., 2010) extended the sampling to tree crowns despite their important proportion in tropical trees volume and mass (Goodman et al.,

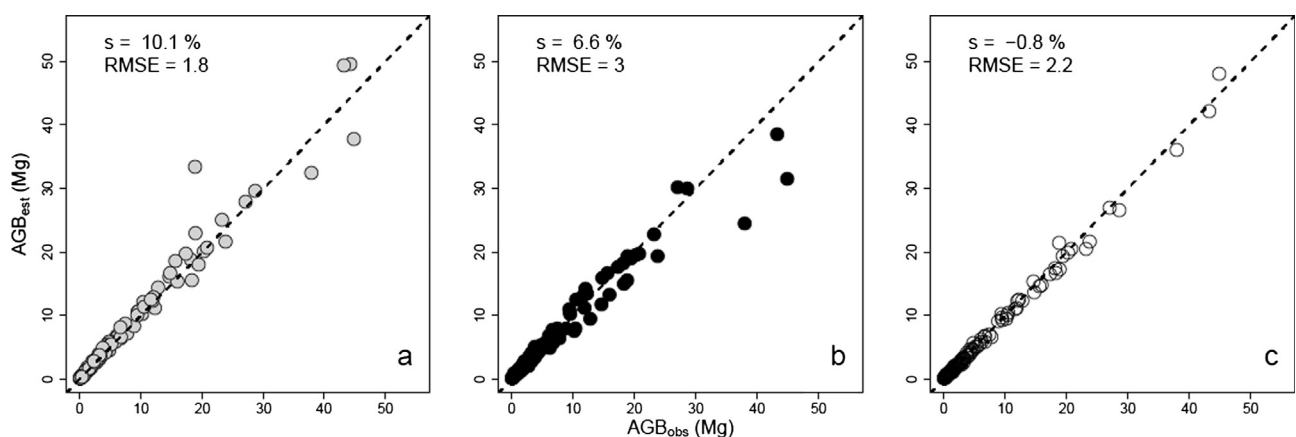


Fig. 2. Scatter plot of the estimated AGB from different WSG sources against field AGB. a = biomass predicted with WSG_{Base} ; b = biomass predicted with WSG_{Dryad} ; c = biomass estimated with WWSG predicted with model 6. The dotted line is the 1:1 line.

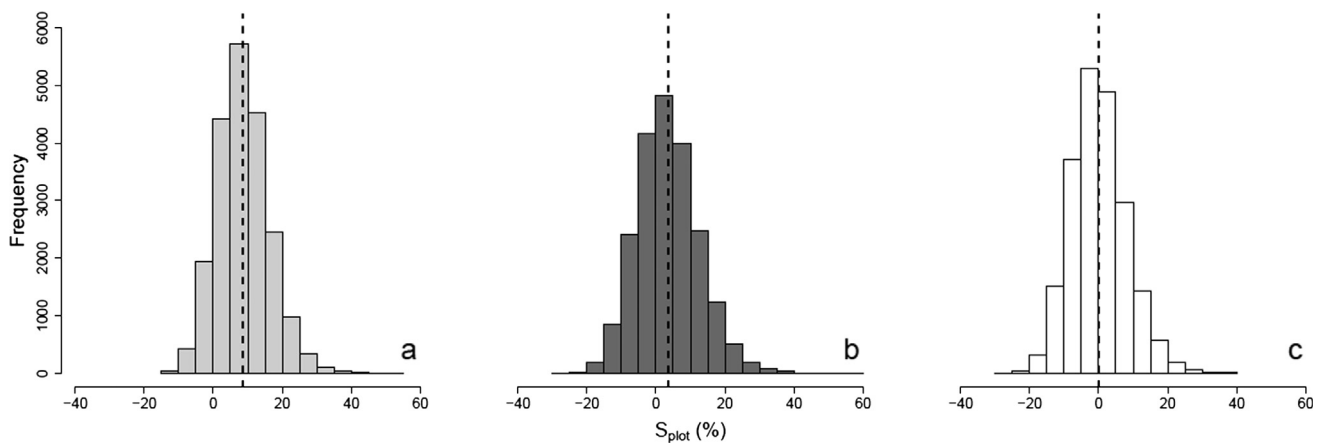


Fig. 3. Frequency distributions of plot-level AGB relative bias (S_{plot} , in%) resulting from the use of different WSG sources: WSG_{Base} (caption a); WSG_{Dryad} (caption b) and WWSG predicted from model 6 (caption c), Dashed vertical lines represent distributions mean.

2014; Ploton et al., 2016). Here, we benefited from a dataset featuring a representative characterization of the specific richness of the sampling area and comprising a significant number of large trees (52% of the dataset with a $DBH > 50$ cm), and we could compute representative estimates of tree-level WSG (ie. WWSG) based on volume-weighted WSG on each tree compartment, from the stump to the crown, using a systematic sampling along the tree. The WWSG was generally lower than the tree basal WSG. This result is explained by the fact that most sampled trees (93% in our study) presented a decreasing WSG upward across tree compartments (Appendix B). Although some species may present the opposite variation pattern (eg. *Macaranga barteri* in our study), a decrease of WSG along the tree vertical profile seems to be a general pattern at the community level (Melo et al., 2005; Sarmiento et al., 2011; Swenson and Enquist, 2008). The WWSG was also found to be lower than species-average WSG derived from Dryad database. Indeed, wood samples gathered in repositories such as Dryad generally originate from the breast height or from the bole (Zanne et al., 2009), hence are subject to the same bias pattern as WSG_{Base} . The difference between WWSG and WSG_{Dryad} (or WSG_{Base}), and ultimately the bias in

tree AGB estimate, is a function of the slope of tree WSG vertical profile but also of the relative volumes of the tree compartments. Interestingly, variations in species WSG vertical profile were to some extent compensated by variations in species morphology (in terms of compartments' relative volumes), leading to more homogeneous distribution of $WWSG_j$. For instance, while *Macaranga barteri* showed an increasing WSG from the stump to the crown, weighting compartments' WSG by compartments' volume led to the typical pattern of $WWSG_j$ variation (Appendix C-a), with a peak at the bole-level and in big size branches followed by a decrease toward small branches. In fact, we differentiated two $WWSG_j$ distribution strategies in the species sampled (Appendix C). In most species, the bole presented the highest WWSG values except *Macaranga barteri*, *Baphia leptobotrys*, *Duboscia macrocarpa* and *Pentaclethra macrophylla* who had highest values in the crown (Appendix C f; m, o). The latter four species were morphologically distinct (Appendix A) with a bole that was under-represented compared to other species.

Our set of predictive models (Table 2) for WWSG were calibrated across a set of 15 tree species in the specific context of semi-deciduous forests in Eastern Cameroun and should be used with caution for other

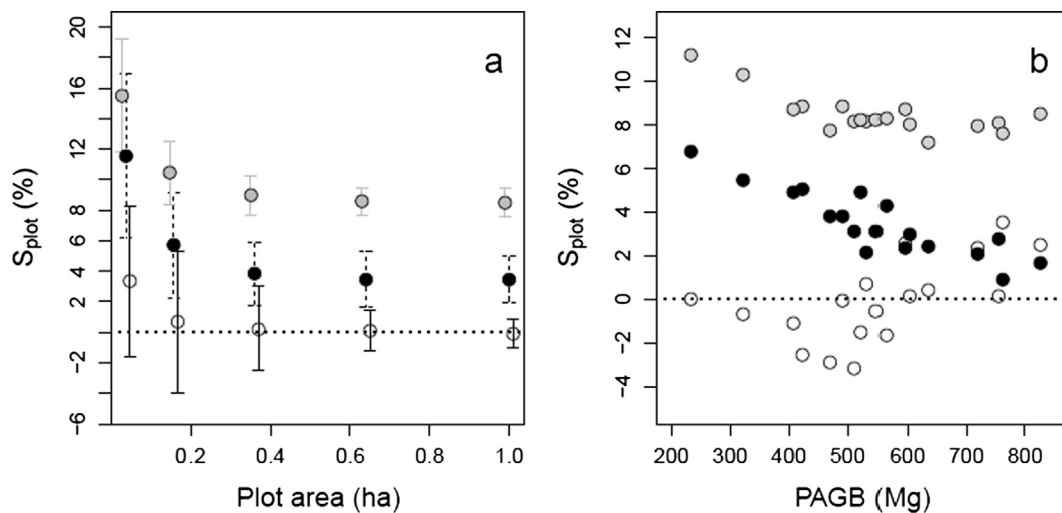


Fig. 4. Plot-level AGB relative bias (S_{plots} %) as a function of plot area (caption a) and plot-level AGB (caption b). In both caption, each dot represents the mean bias of a given simulated plot over 1000 realizations. Simulated plot AGB predictions ($PAGB_{sim}$) were made using different WSG sources: WSG_{Base} (solid grey circles) WSG_{Dryad} (solid black circle) and WWSG predicted from model 6 (solid white circles).

tree species and sites. However, they provide good insights into the feasibility of *WWSG* prediction as our best models based on WSG_{Base} (model 3) explained as much as 81% of the individual *WWSG* variation and the one based on WSG_{Dryad} (model 6) explained as much as 72% of the variation. The significant effects of the variables *DBH* and S_m in the models suggest that the overall structure and size of trees should be taken into account when estimating *WWSG*. Other factors not considered in this study could explain the remaining variability. Improvement of wood density estimation could for instance necessitate a better accounting of tree life history (De Castro et al., 1993).

Depending on the *WSG* source used, we obtained an overestimation of tree-level AGB of 10% on average when using WSG_{Base} and 7% on average when using WSG_{Dryad} , whereas using *WWSG* predicted from model 6 yielded an average bias of only - 1%. It is worth stressing that using WSG_{Dryad} does not induce a bias when tree AGB is estimated with a biomass allometry model calibrated on WSG_{Dryad} (such as the pan-tropical biomass model of Chave et al. 2014), because model's coefficients account for the variation pattern between WSG_{Dryad} and *WWSG*. However, this bias would propagate to AGB estimates when simply converting volume to biomass, as it is the case when one uses terrestrial LiDAR technologies to derive trees and forest AGB. Systematic differences in trees AGB derived from the two methods (ie. terrestrial LiDAR – based vs allometry model-based) may partially be attributed to this phenomenon (as in Gonzalez de Tanago et al., 2018).

Propagating tree-level AGB bias to the plot-level, we observed that plot-level bias (S_{plot}) was a function of plot AGB and plot size. S_{plot} increased as plot AGB and size decreased, although AGB overestimation was systematic with both WSG_{Base} and WSG_{Dryad} . At the 0.04 ha scale, the error on plot AGB estimate induced using WSG_{Dryad} was higher than 11% on average. We thus proposed a solution to correct the errors linked to plot size and complexity as encountered in LiDAR studies (Bouvier, 2015; Rafael M et al., 2017) because using *WWSG* values predicted from our model 6 significantly reduces the plot-level bias to 3% in small plots (0.04 ha) and 0.01% in 1 ha plots. The fact that bias propagation is dependent on plot structure implies that the use of

uncorrected WSG_{Base} and WSG_{Dryad} , for converting tree volumes into biomass in broader scale studies e.g. within National Forest Inventories or REDD+ scheme, will produce spatially structured errors, with different forest types having different overestimation levels.

5. Conclusion

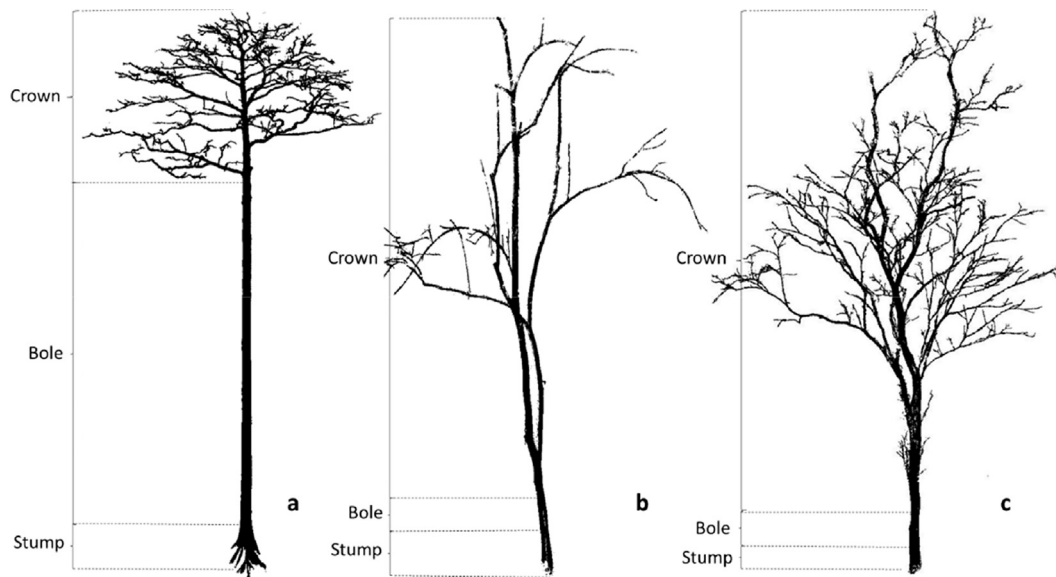
In this study, species-level average *WWSG* was generally lower than the *WSG* values recorded from Dryad and the basal *WSG* collected in the field. It was also shown that linear models incorporating few variables *i.e.* general tree size and structure, especially S_m and *DBH*, allow to accurately predict tree level *WWSG*. Therefore, estimating AGB with predicted *WWSG* produced less biased estimates at the tree level relative to WSG_{Base} and WSG_{Dryad} , which generally overestimate AGB. At the plot level, the bias yielded when predicting AGB with WSG_{Base} and WSG_{Dryad} was influenced by the size and total AGB of the plot; there was a decreasing trend as the overall plot size and AGB increases. Predicted *WWSG* values from our study produces plot-level estimation that are both less biased and less sensitive to forest structure when converting tree volume into biomass.

Acknowledgements

This research has received funding from the Global Environment Fund under the World Bank's grant No. TF010038, sub-component 2b of the COMIFAC Regional REDD+ Project "Establishment of allometric equations for the Congo Basin forests" a sub-component implemented by the ONFI/TEREA/Nature+ consortium. Adeline Fayolle and Adrien Peroches were involved in the establishment and follow-up of the sampling protocol and we also thank them for comments on earlier versions of the paper. We are very grateful to the Alpicam-Grumcam company and in particular D. Bastin, M. Ramoni and C. Pizzutto, for their constant logistics support during this and previous studies. The authors thank anonymous reviewers for comments that helped improve the quality of the paper.

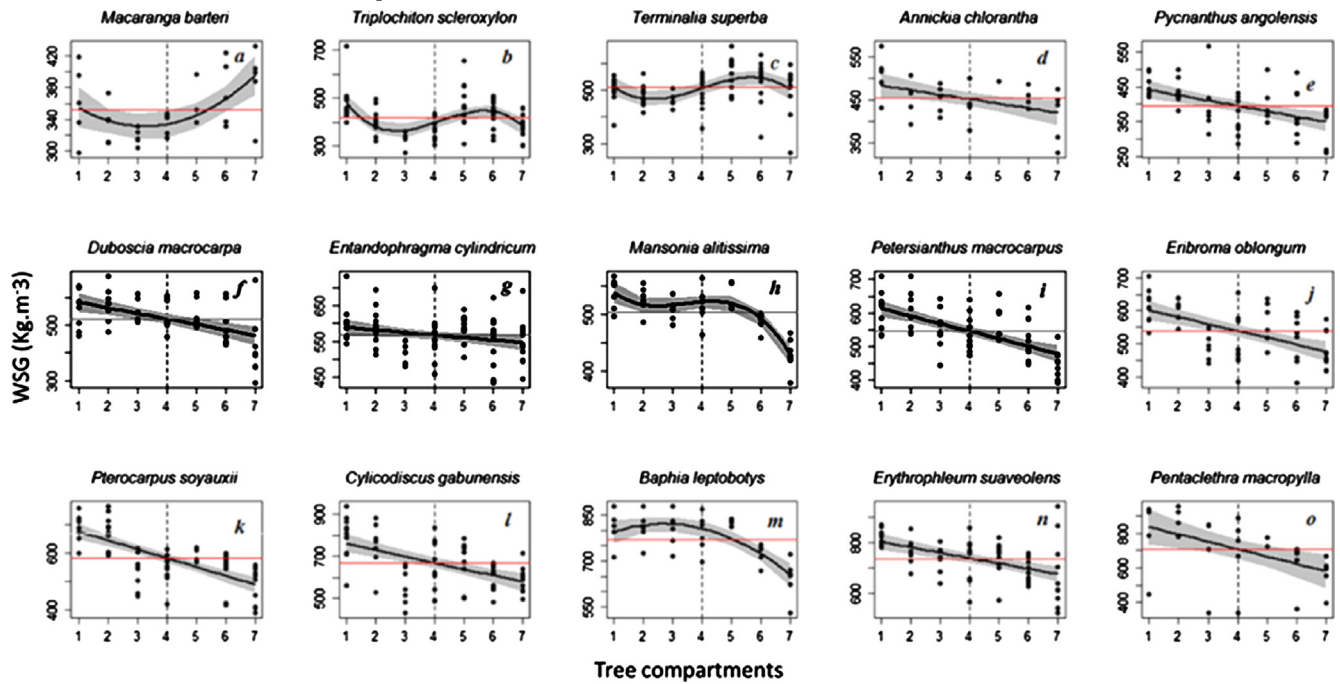
Appendix A

Different tree morphologies presented by the species sampled regarding the proportion of the bole. a = tall-bole species (*Terminalia superba*); b and c = short-bole species (*Duboscia macrocarpa* and *Baphia leptobotrys* respectively). Tree images are extracted from T-LiDAR scans.



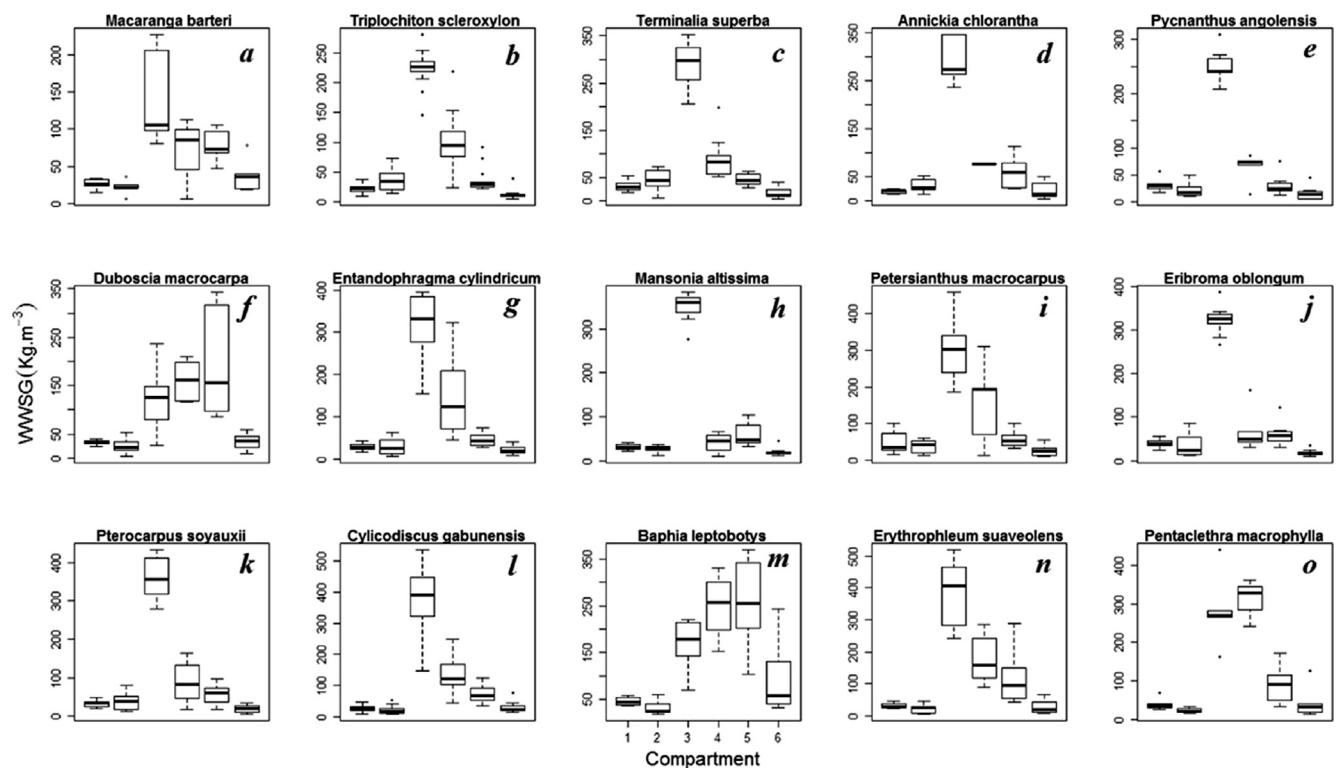
Appendix B

Vertical WSG profiles of the 15 species; X-axis shows the levels along the tree where wood samples were collected (1 = stump base; 2 = lower portion of the bole with buttresses, 3 = bole; 4 = upper portion of the bole before the first main branches, 5 = Big branches, 6 = medium branches, 7 = small branches), Y-axis shows the WSG. The black line represents the WSG best fit profile with 95% C.I (grey); the horizontal line represents the species' mean WSG and the dotted line represents the delimitation between the stem and crown.



Appendix C

WWSG distribution between woody compartments. 1 = stump; 2 = lower portion of the bole with buttresses, 3 = bole; 4 = big branches, 5 = middle sized branches, 6 = small branches. *Macaranga barteri*, *Duboscia macrocarpa* and *Baphia leptobotys* and *Pentaclethra macrophylla* present a WWSG profile different from other species; the highest WWSG values are observed in the branches whereas in other species the highest values are on the bole.



References

- Alvaro, L.S., Gonzalez De Tanago, J., Bartholomeus, H., Herold, M., Avitabile, V., Raunonen, P., Martius, C., Goodman, R., Disney, M., Manuri, S., Burt, A., Calders, K., 2017. Above-ground Biomass Assessment of Large Trees with Terrestrial LiDAR and 3D Architecture Models.
- Bastin, J.-F., Barbier, N., Réjou-Méchain, M., Fayolle, A., Gourlet-Fleury, S., Maniatis, D., de Haulleville, T., Baya, F., Beekman, H., Beina, D., Couteron, P., Chuyong, G., Dauby, G., Doucet, J.-L., Droissart, V., Dufréne, M., Ewango, C., Gillet, J.F., Gonmadje, C.H., Hart, T., Kavali, T., Kenfack, D., Libalah, M., Malhi, Y., Makana, J.-R., Péliissier, R., Ploton, P., Serckx, A., Sonké, B., Stewart, T., Thomas, D.W., De Cannière, C., Bogaert, J., 2015a. Seeing Central African forests through their largest trees. *Sci. Rep.* 5, 1–8. <http://dx.doi.org/10.1038/srep13156>.
- Bastin, J., Fayolle, A., Tarelkin, Y., Van Den Bulcke, J., De Haulleville, T., Mortier, F., Beeckman, H., Van Acker, J., Serckx, A., Bogaert, J., De Cannière, C., 2015b. Wood specific gravity variations and biomass of central African tree species: The simple choice of the outer wood. *PLoS One* 10, 1–16. <http://dx.doi.org/10.1371/journal.pone.0142146>.
- Bouvier, M., 2015. Influence of sampling design parameters on biomass predictions derived from airborne lidar. 23–26.
- Calders, K., Newnham, G., Burt, A., Murphy, S., Raunonen, P., Herold, M., Culvenor, D., Avitabile, V., Disney, M., Armston, J., Kaasalainen, M., 2015. Nondestructive estimates of above-ground biomass using terrestrial laser scanning. *Methods Ecol. Evol.* 6, 198–208. <http://dx.doi.org/10.1111/2041-210X.12301>.
- Chave, J., Condit, R., Aguilar, S., Hernandez, A., Lao, S., Perez, R., 2004. Error propagation and scaling for tropical forest biomass estimates. 409–420. <http://doi.org/10.1098/rstb.2003.1425>.
- Chave, J., Coomes, D., Jansen, S., Lewis, S.L., Swenson, N.G., Zanne, A.E., 2009. Towards a worldwide wood economics spectrum. *Ecol. Lett.* 12 (4), 351–366.
- Chave, J., Réjou-Méchain, M., Búrquez, A., Chidumayo, E., Colgan, M.S., Delitti, W.B.C., Duque, A., Eid, T., Fearnside, P.M., Goodman, R.C., Henry, M., Martínez-Yrizar, A., Mugasha, W.A., Muller-Landau, H.C., Mencuccini, M., Nelson, B.W., Ngomanda, A., Nogueira, E.M., Ortiz-Malavassi, E., Péliissier, R., Ploton, P., Ryan, C.M., Saldarriaga, J.G., Vieilledent, G., 2014. Improved allometric models to estimate the aboveground biomass of tropical trees. *Glob. Chang. Biol.* 20, 3177–3190. <http://dx.doi.org/10.1111/gcb.12629>.
- Daphné, H., Philippe, L., 2014. Qgis 08: Géoréférencement d'un raster. Gembloux.
- De Castro, F., Williamson, G.B., Jesus, R.M., 1993. Radial variation in wood specific gravity of *Joannesia princeps*: the roles of age and diameter. *Biotropica* 25, 176–182.
- Deng, X., Zhang, L., Lei, P., Xiang, W., Yan, W., Deng, X., Zhang, L., Lei, P., Xiang, W., Yan, W., 2014. Variations of wood basic density with tree age and social classes in the axial direction within *Pinus massoniana* stems in Southern China To cite this version: Variations of wood basic density with tree age and social classes in the axial direction within. *Ann. For. Sci.* 71, 505–516. <http://dx.doi.org/10.1007/s13595-013-0356-y>.
- Disney, M.I., Boni Vicari, M., Burt, A., Calders, K., Lewis, S.L., Raunonen, P., Wilkes, P., 2018. Weighing trees with lasers: advances, challenges and opportunities. *Interface Focus* 8, 20170048. <http://dx.doi.org/10.1098/rsfs.2017.0048>.
- Fayolle, A., Picard, N., Doucet, J.-L., Swaine, M., Bayol, N., Bénédet, F., Gourlet-Fleury, S., 2014. A new insight in the structure, composition and functioning of central African moist forests. *For. Ecol. Manage.* 329, 195–205. <http://dx.doi.org/10.1016/j.foreco.2014.06.014>.
- Ferraz, A., Saatchi, S., Mallet, C., Meyer, V., 2016. Lidar detection of individual tree size in tropical forests. *Remote Sens. Environ.* 183, 318–333. <http://dx.doi.org/10.1016/j.RSE.2016.05.028>.
- Gibbs, H.K., Brown, S., Niles, J.O., Foley, J.A., 2007. Monitoring and estimating tropical forest carbon stocks: making REDD a reality. *Environ. Res. Lett.* 2, 45023. <http://dx.doi.org/10.1088/1748-9326/2/4/045023>.
- Gonzalez de Tanago, J., Lau, A., Bartholomeus, H., Herold, M., Avitabile, V., Raunonen, P., Martius, C., Goodman, R.C., Disney, M., Manuri, S., Burt, A., Calders, K., 2018. Estimation of above-ground biomass of large tropical trees with terrestrial LiDAR. *Methods Ecol. Evol.* 9, 223–234. <http://dx.doi.org/10.1111/2041-210X.12904>.
- Goodman, R.C., Phillips, O.L., Baker, T.R., 2014. The importance of crown dimensions to improve tropical tree biomass estimates. *Ecol. Appl.* 24, 680–698.
- Gourlet-Fleury, S., Mortier, F., Fayolle, A., Baya, F., Ouédraogo, D., Bénédet, F., Picard, N., 2013. Tropical forest recovery from logging: a 24 year silvicultural experiment from Central Africa. *Philos. Trans. R. Soc. B Biol. Sci.* 368.
- Hackenberg, J., Wassenberg, M., Spiecker, H., Sun, D., 2015. Non destructive method for biomass prediction combining TLS derived tree volume and wood density. *Forests* 6, 1274–1300. <http://dx.doi.org/10.3390/f6041274>.
- Henry, M., Besnard, A., Asante, W.A., Eshun, J., Adu-Bredu, S., Valentini, R., Bernoux, M., Saint-André, L., 2010. Wood density, phytomass variations within and among trees, and allometric equations in a tropical rainforest of Africa. *For. Ecol. Manage.* 260, 1375–1388. <http://dx.doi.org/10.1016/j.foreco.2010.07.040>.
- Joseph, S., Herold, M., Sunderland, W.D., Verchot, L.V., 2013. REDD + readiness: Early insights on monitoring, reporting and verification systems of project developers. *Environ. Res. Lett.* 8. <http://dx.doi.org/10.1088/1748-9326/8/3/034038>.
- Letouzey, R., 1968. Etude phytogéographique du Cameroun. In: *Encyclopédie Biologique*, vol. 69. p. 511.
- Libalah, Moses B., Droissart, Vincent, Sonké, Bonaventure, Kamdem, Gyslene, Kamdem, Narcisse, Mofack, Gislain II, Péliissier, Raphaël, Ploton, Pierre, Réjou-Méchain, Maxime, Lewis, Simon L., Momo, Stéphane Takoudjou, Texier, Nicolas, Zebazé, Donatien, Barbier, Nicolas, Couteron, Pierre, 2018. Soil and climate gradients complementarily influence the abundance of scarce and abundant tree species in Central African moist forests. *J. Veg. Sci.* 33pp (in prep).
- Maniatis, D., Malhi, Y., Saint André, L., Mollicone, D., Barbier, N., Saatchi, S., Henry, M., Tellier, L., Schwartzberg, M., White, L., 2011. Evaluating the potential of commercial forest inventory data to report on forest carbon stock and forest carbon stock changes for REDD+ under the UNFCCC. *Int. J. For. Res.* 2011, 1–13. <http://dx.doi.org/10.1155/2011/134526>.
- Melo, E., Walker, B., Fearnside, P.M., 2005. Wood density in dense forest in central Amazonia, Brazil. *For. Ecol. Manage.* 208, 261–286. <http://dx.doi.org/10.1016/j.foreco.2004.12.007>.
- Momo, T.S., Ploton, P., Sonké, B., Hackenberg, J., Griffon, S., de Coligny, F., Kamdem, N.G., Libalah, M., Mofack, G.I., Le Moguédec, G., Péliissier, R., Barbier, N., 2017. Using Terrestrial Laser Scanning data to estimate large tropical trees biomass and calibrate allometric models: a comparison with traditional destructive approach. *Methods Ecol. Evol.* <http://dx.doi.org/10.1111/2041-210X.12933>.
- Nock, C.A., Geihofer, D., Grabner, M., Baker, P.J., 2009. Wood density and its radial variation in six canopy tree species differing in shade-tolerance in western Thailand. *Ann. Bot.* 104, 297–306. <http://dx.doi.org/10.1093/aob/mcp118>.
- Osazuwa-Peters, O.L., Wright, S.J., Zanne, A.E., 2014. Radial variation in wood specific gravity of tropical tree species differing in shade-mortality strategies. *Am. J. Bot.* 101, 803–811. <http://dx.doi.org/10.3732/ajb.1400040>.
- Pardé, J., Bouchon, J., 1988. Dendrométrie, Agroparistech.
- Picard, N., Boyemba Bosela, F., Rossi, V., 2015. Reducing the error in biomass estimates strongly depends on model selection. *Ann. For. Sci.* 72, 811–823. <http://dx.doi.org/10.1007/s13595-014-0434-9>.
- Picard, N., Saint-andré, L., Henry, M., 2012. Manuel de construction d' équations allométriques pour l' estimation du volume et la biomasse des arbres.
- Ploton, P., Barbier, N., Couteron, P., Antin, C.M., Ayyappan, N., Balachandran, N., Barathan, N., Bastin, J.-F., Chuyong, G., Dauby, G., Droissart, V., Gastellu-Etchegorry, J.-P., Kamdem, N.G., Kenfack, D., Libalah, M., Mofack, G., Momo, S.T., Pargal, S., Petronelli, P., Proisy, C., Réjou-Méchain, M., Sonké, B., Texier, N., Thomas, D., Verley, P., Zebaze Dongmo, D., Berger, U., Péliissier, R., 2017. Toward a general tropical forest biomass prediction model from very high resolution optical satellite images. *Remote Sens. Environ.* 200, 140–153. <http://dx.doi.org/10.1016/j.rse.2017.08.001>.
- Ploton, P., Barbier, N., Momo, S.T., Rejou-Mechain, M., Boyemba Bosela, F., Chuyong, G., Dauby, G., Droissart, V., Fayolle, A., Calisto Goodman, R., Henry, M., Guy Kamdem, N., Kateambo Mukirania, J., Kenfack, D., Libalah, M., Ngomanda, A., Rossi, V., Sonke, B., Texier, N., Thomas, D., Zebaze, D., Couteron, P., Berger, U., Péliissier, R., 2016. Closing a gap in tropical forest biomass estimation: Taking crown mass variation into account in pantropical allometries. *Biogeosciences* 13, 1571–1585. <http://dx.doi.org/10.5194/bg-13-1571-2016>.
- Pohlert, T., 2016. The Pairwise Multiple Comparison of Mean Ranks Package (PMCMR). CRAN. <https://doi.org/http://cran.ms.unimelb.edu.au/web/packages/PMCMR/vignettes/PMCMR.pdf>.
- Rafael, M. N.-C., Eduardo, G.-F., Jorge, G.-G., Carlos J Ceacero, R., Rocío, H.-C., 2017. Impact of plot size and model selection on forest biomass estimation using airborne LiDAR: A case study of pine plantations in southern Spain. *J. For. Sci.* 63, 88–97. <https://doi.org/10.17221/86/2016-JFS>.
- Ramanananantoandro, T., Rafidimanantsoa, H.P., Ramanakoto, M.F., 2015. Forest above-ground biomass estimates in a tropical rainforest in Madagascar: new insights from the use of wood specific gravity data. *J. For. Res.* 26, 47–55. <http://dx.doi.org/10.1007/s11676-015-0029-9>.
- RStudio Team, -, 2016. RStudio: Integrated Development for R. [Online] RStudio, Inc., Boston, MA URL <http://www.rstudio.com> RStudio, Inc., Boston, MA. <https://doi.org/10.1007/978-81-322-2340-5>.
- Sarmiento, C., Patiño, S., Timothy Paine, C.E., Beauchêne, J., Thibaut, A., Baraloto, C., 2011. Within-individual variation of trunk and branch xylem density in tropical trees. *Am. J. Bot.* 98, 140–149. <http://dx.doi.org/10.3732/ajb.1000034>.
- Slik, J.W.F., Paoli, G., McGuire, K., Amaral, I., Barroso, J., Bastian, M., Blanc, L., Bongers, F., Boundja, P., Clark, C., Collins, M., Dauby, G., Ding, Y., Doucet, J.L., Eler, E., Ferreira, L., Forshed, O., Fredriksson, G., Gillet, J.F., Harris, D., Leal, M., Laumonier, Y., Malhi, Y., Mansor, A., Martin, E., Miyamoto, K., Araujo-Murakami, A., Nagamasu, H., Nilus, R., Nurtjahya, E., Oliveira, Á., Onrizal, O., Parada-Gutierrez, A., Permana, A., Poorter, L., Poulsen, J., Ramirez-Angulo, H., Reitsma, J., Rovero, F., Rozak, A., Sheil, D., Silva-Espejo, J., Silveira, M., Spironeo, W., ter Steege, H., Stewart, T., Navarro-Aguilar, G.E., Sunderland, T., Suzuki, E., Tang, J., Theilade, I., van der Heijden, G., van Valkenburg, J., Van Do, T., Vilanova, E., Vos, V., Wich, S., Wöll, H., Yoneda, T., Zang, R., Zhang, M.G., Zweifel, N., 2013. Large trees drive forest aboveground biomass variation in moist lowland forests across the tropics. *Glob. Ecol. Biogeogr.* 22, 1261–1271. <http://dx.doi.org/10.1111/geb.12092>.
- Stovall, A.E.L., Vorster, A.G., Anderson, R.S., Evangelista, P.H., Shugart, H.H., 2017. Non-destructive aboveground biomass estimation of coniferous trees using terrestrial LiDAR. *Remote Sens. Environ.* 200, 31–42. <http://dx.doi.org/10.1016/j.rse.2017.08.013>.

- Swenson, N.G., Enquist, B.J., 2008. The relationship between stem and branch wood specific gravity and the ability of each measure to predict leaf area. *Am. J. Bot.* 95, 516–519. <http://dx.doi.org/10.3732/ajb.95.4.516>.
- Vieilledent, G., Vaudry, R., Andriamanohisoa, S.F.D., Rakotonarivo, O.S., Randrianasolo, H.Z., Razafindrab, H.N., Rakotoarivony, C.B., Ebeling, J., Rasamoelina, M., 2012. A universal approach to estimate biomass and carbon stock in tropical forests using generic allometric models. *Ecol. Appl.* 22, 572–583.
- Vincke, D., 2011. Elaboration d' une méthodologie d'estimation de la biomasse ligneuse aérienne de populations d' espèces commerciales du Sud-Est Sud Est du Cameroun. Gembloux agro bio tech, Université de Liège.
- Wassenberg, M., Chiu, H.S., Guo, W., Spiecker, H., 2015. Analysis of wood density profiles of tree stems: incorporating vertical variations to optimize wood sampling strategies for density and biomass estimations. *Trees – Struct. Funct.* 29, 551–561. <http://dx.doi.org/10.1007/s00468-014-1134-7>.
- Williamson, G.B., Wiemann, M.C., 2010. Measuring wood specific gravity...Correctly. *Am. J. Bot.* 97, 519–524. <http://dx.doi.org/10.3732/ajb.0900243>.
- Zanne, A.E., Lopez-Gonzalez, G., Coomes, D.A., Ilic, J., Jansen, S., Lewis, S.L., Miller, R.B., Swenson, N.G., Wiemann, M.C., Chave, J., Zanne, A.E., Lopez-Gonzalez, G., Coomes, D.A., Ilic, J., Jansen, S., Lewis, S.L., Miller, R.B., Swenson, N.G., Wiemann, M.C., Chave, J., 2009. Global Wood Density Database. <https://doi.org/10.5061/DRYAD.234/1>.